Power spectrum and fractal dimension of laser backscattering from the ocean

James H. Churnside and James J. Wilson

Earth System Research Laboratory, National Oceanic and Atmospheric Administration, 325 Broadway, Boulder, Colorado, 80305

Received January 6, 2006; accepted June 9, 2006; posted June 26, 2006 (Doc. ID 67062)

We flew an airborne lidar perpendicular to the coastline along straight-line transects that varied in length between 230 and 280 km. The sample spacing was ~3 m, so we sampled almost five decades of spatial scales. Except for the return from right at the surface, the power spectra of backscattered power had a power-law dependence on spatial frequency, with a slope of ~1.49. This corresponds to a fractal dimension of 1.76. This implies that the distribution is not as patchy as that of a purely turbulent process.

OCIS codes: 010.3640, 010.4450, 280.7060, 290.7050.

1. INTRODUCTION

In July 2003, we flew the National Oceanic and Atmospheric Administration (NOAA) Fish lidar in a series of long, straight transects off the coast of Oregon and Washington. These transects were long enough that we could sample a range of spatial scales of almost five decades in ~45 min. The wide range of spatial scales suggested an investigation into whether the lidar return exhibited fractal characteristics over some part of this range. We were particularly interested to see if the distribution of scattering particles measured by the lidar had a power spectrum characteristic of turbulent mixing over some range of spatial scales.

There are several techniques to investigate the fractal characteristics of a data set, but the one that seems most appropriate for our work involves finding the power spectrum of a time series.[1] A fractal process is characterized by a power-law spectrum of the form

$$S = f^{-\beta}, \tag{1}$$

where f is the frequency and β is the slope of the spectrum on a log–log plot. In our case, the temporal frequency is converted into a more meaningful spatial frequency by using the speed of the aircraft. For a one-dimensional measurement, the fractal dimension (Hausdorff–Besicovitch) is inferred from the slope through the relationship

$$D = 2.5 - 0.5\beta. \tag{2}$$

There have been several studies into the fractal nature of light scattered from the ocean surface. Zosimov and Naugolnykh[2] measured the number of laser glints from a ship. They found a spectral slope of 0.86 over a frequency range of 0.02–0.2 Hz, which corresponds to spatial wavelengths of 40–400 m. Shaw and Churnside[3] made a similar measurement from a stationary platform and found a spectral slope of 0.62 over a frequency range of 0.001–0.3 Hz. These frequencies are below the frequency of the dominant wind waves, and this range roughly corresponds to the range in Zosimov and Naugolnykh. At frequencies (1.5–15 Hz) higher than that of the dominant wind waves, Shaw and Churnside observed a slope of 1.45.

There have also been studies of the fractal nature of light scattered from the water volume. Lovejoy *et al.*[4] measured scattered solar radiance from the ocean in eight channels, and over spatial scales from 14 m to 110 km. The spectral slope for all channels was ~1.25, at least for scales greater than 100 m.

2. LIDAR SYSTEM AND OPERATIONS

The NOAA Fish lidar is a backscatter lidar under development for the detection of fish schools, and is described in detail elsewhere.[5–8] During the flights described in this paper, the system transmitted ~120 mJ of linearly polarized, green (532 nm) light per pulse at a rate of 30 pulses/s. During the day, the beam divergence (full width) was ~17 mrad. At night, this was increased to ~50 mrad.

The system receiver recorded the temporal evolution of the return from each pulse in the linear polarization perpendicular to that of the transmitted pulse. The cross polarization was chosen to provide the best contrast between fish and small particles in the water. The field of view of the receiver telescope was matched to the transmitted beam divergence. The detector was a photomultiplier tube equipped with an interference filter to reduce background light. An amplifier with a logarithmic response compressed four decades of dynamic range into the 8 bit range of the digitizer, which sampled the signal at a rate of 1 GHz. The signal is a combination of the scattering from suspended sediments, phytoplankton, zooplankton, and fish in relation to the volume backscatter coefficient and depolarization of each.

The system computer recorded the lidar return, global positioning system position, and the gain on the photomultiplier tube. In processing, the response of the amplifier and the gain of the photomultiplier were used to cal-

culate the photocathode current for each sample. This current is directly proportional to the volume backscatter coefficient $\beta(\pi)$ at the distance corresponding to the time delay for each sample. These distances were converted to depth by locating the large surface return in each pulse waveform and counting samples from there. Each additional sample corresponds to ~0.11 m of depth.

Each flight began near the coast and went due west out almost to 128°W, where the plane turned around and followed the same line back (Fig. 1). This was done during the day and at night for each of the five lines. Flight altitude was ~300 m, and flight speed was 90 ± 4 m s^{-1}, so the lidar pulses were separated by ~3 m along the flight track. At this altitude, the lidar spot diameter on the surface was ~5 m during the daytime flights and ~15 m at night. The flight tracks varied in length from ~230 to 280 km, so we sampled almost five decades of horizontal scales. The time to cover each transect varied between 43 min for the shortest line and 52 min for the longest, so we would expect little aliasing of temporal variability into the inferred spatial variability.

The data were separated by direction of flight (westbound or eastbound), time of day (daytime or nighttime), and latitude to obtain a total of 20 transects. For each transect, we extracted the magnitude of the lidar return from depths of 0, 5, 10, 15, and 20 m, for a total of 100 time series of data. We calculated the power spectrum of each of these time series and estimated its slope by using a least-squares fit to the plot of the logarithm of the power spectrum against the logarithm of the spatial scale over the spatial scale range from 10^{-4} to 0.1 rad m^{-1}. At lower spatial frequencies, the spectra are noisy because there are relatively few samples that contribute. At higher spatial frequencies, the data are occasionally contaminated by system noise because the lidar signal is small; this effect is larger during the daytime flights when the lidar signal is noisier.

3. RESULTS

The first result is that the power spectra for the depths of 5–20 m are well approximated by a power law over most of the range of spatial frequencies. The typical spectra of Fig. 2 show that the power law holds until the white instrument noise level is reached. Nighttime data are generally cleaner than daytime data, and data from deeper in the water column tend to be noisier than data from closer to the surface. The data from deeper in the water are also at lower levels because of attenuation in the water, but the slopes are generally similar.

The surface data can be different. While the surface data from 45°N are similar to the data from other depths, the data from other latitudes can be very different. Figure 3 shows a spectrum that does not have a clear power-law dependence, and the slope over the range of spatial scales we are using is much less than at other depths. However, the spectrum appears to have a power-law component at lower frequencies and a broad peak centered at ~0.1 m^{-1}. This frequency corresponds to a wavelength of ~60 m; a surface wave with this wavelength would have a period of ~6 s.

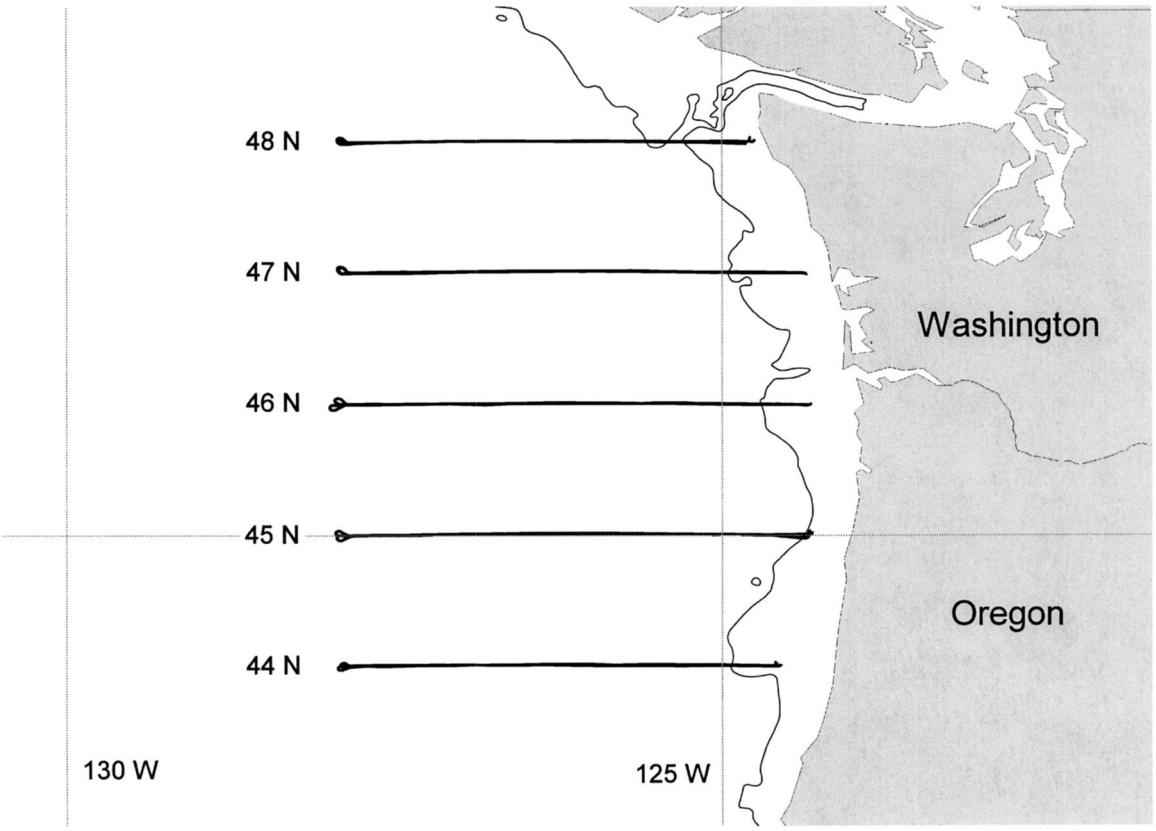

Fig. 1. Flight tracks off the coast of Oregon and Washington along integer latitude lines from 44°N to 48°N. Location of the shelf break (200 m isobath) is shown off the coastline.

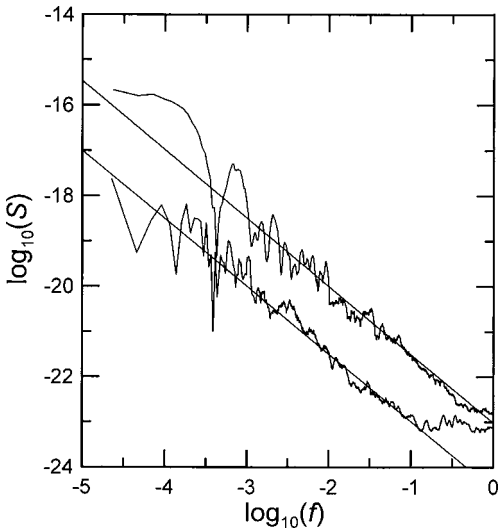

Fig. 2. Logarithm of power spectrum of lidar return S as a function of spatial frequency f along 45°N latitude for a depth of 20 m during the day (lower curve) and a depth of 10 m the same night (upper curve). Also shown are the linear fits with slopes of −1.47 and −1.52, respectively.

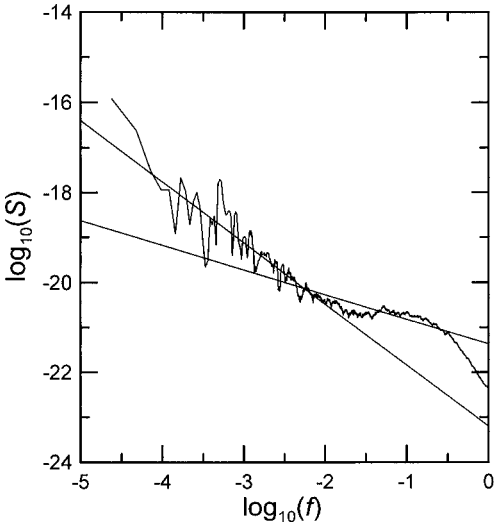

Fig. 3. Logarithm of power spectrum of lidar return S as a function of spatial frequency f along 44°N latitude for a depth of 0 m at night. The shallower line is the fit from −4 to −1 with a slope of −0.51, and the steeper line is the fit from −4 to −2 with a slope of −1.36.

The 6 s period can be compared with the average wave period recorded by buoys in the vicinity.[9] We note that the lidar data were collected between 6:12 and 7:00 UTC on July 10 along 44°N. The nearest NOAA buoys are number 46050 at 44.62°N, 124.53°W and number 46015 at 42.75°N, 124.85°W. The average wave periods reported by the first buoy were 5.3 s at 6:00 and 5.4 s at 7:00. The second buoy reported 6.6 s at 6:00 and 6.2 s at 7:00. These values suggest that the peak in the spectrum is an effect of surface waves.

The measured spectral slopes are presented in Table 1 for each of the 100 time series. The average statistical uncertainty in the slope was ~0.005, with the largest uncertainty less than 0.01. The mean slope, neglecting surface values, was 1.49±0.03. Table 2 lists the mean slopes for various subsets of the data. We used the Student's t-test to test the hypotheses that various combinations of slopes were from distributions with different mean values, using a confidence level of 0.05.

In the first test, we investigated the values by depth. Figure 4 suggests that the surface values might be significantly different from the values at different depths. The t-test results show that the surface results are different from the results at each of the other depths, but we cannot say that the results from any two other depths are different from each other. With this result, we neglected the surface results in comparing day values with night values and found a small, but statistically significant, difference

Table 1. Spectral Slopes by Latitude, Time of Day, Flight Direction, and Depth

			Slope (m)				
Latitude (deg)	Time	Direction	0	5	10	15	20
44	Day	East	0.64	1.53	1.41	1.45	1.47
44	Day	West	0.95	1.63	1.51	1.32	1.47
44	Night	East	0.51	1.58	1.54	1.42	1.39
44	Night	West	0.53	1.50	1.62	1.48	1.40
45	Day	East	1.26	1.39	1.40	0.97	1.15
45	Day	West	1.48	1.72	1.49	1.59	1.47
45	Night	East	1.75	1.71	1.63	1.67	1.86
45	Night	West	1.21	1.45	1.52	1.40	1.36
46	Day	East	1.15	1.42	1.36	1.37	1.37
46	Day	West	1.13	1.54	1.57	1.60	1.37
46	Night	East	1.13	1.38	1.37	1.48	1.66
46	Night	West	1.14	1.44	1.44	1.56	1.59
47	Day	East	0.53	1.37	0.83	1.04	0.92
47	Day	West	0.55	1.51	1.15	0.97	0.88
47	Night	East	0.65	1.62	1.52	1.42	1.20
47	Night	West	0.40	1.66	1.44	1.56	1.57
48	Day	East	1.09	1.72	1.70	1.80	1.61
48	Day	West	1.23	1.64	1.72	1.72	1.65
48	Night	East	0.48	1.66	1.74	1.96	1.91
48	Night	West	1.05	1.68	1.65	1.86	1.77

Table 2. Mean Slope and Uncertainty in Mean for Day and Night (Neglecting Surface) by Depth and by Latitude (Neglecting Surface)

Condition	Mean	Uncertainty
Day	1.42	0.04
Night	1.57	0.03
0 m	0.94	0.08
5 m	1.56	0.03
10 m	1.48	0.05
15 m	1.48	0.06
20 m	1.45	0.06
44°N	1.48	0.02
45°N	1.49	0.06
46°N	1.47	0.03
47°N	1.29	0.07
48°N	1.74	0.03

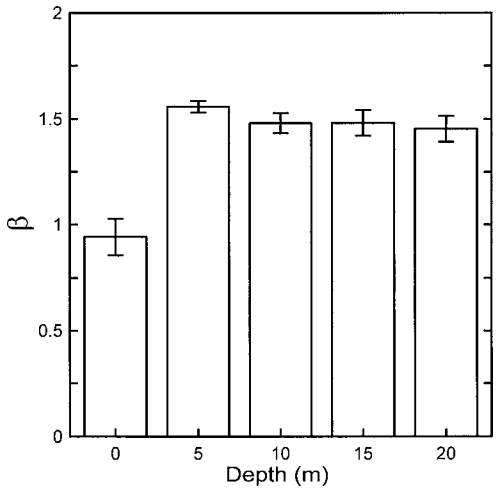

Fig. 4. Depth dependence of power spectral slopes (from Table 2).

between day and night (Fig. 5). Comparing the various latitudes (Fig. 6) (also neglecting surface values), we found the data from 48°N to be significantly different from each of the other transects. The data from 44°N, 45°N, and 46°N are not different. The data from 47°N are interesting; at the confidence level of 0.05, they are different from the southern three lines, but they are not different at a confidence level of 0.02.

4. DISCUSSION

From the measured slope of $\beta=1.49$, we infer an average fractal dimension of $D=1.76$. This implies that the larger scales are more dominant than would be the case for random white noise ($\beta=0, D=2.5$) or $1/f$ noise ($\beta=1.0, D=2.0$), but less dominant than for turbulence within the inertial subrange ($\beta=1.67, D=1.67$) or a Brownian process ($\beta=2.0, D=1.5$). In other words, the lidar scattering from below the surface is patchier than white noise or $1/f$ noise, but not as patchy as turbulence or Brownian motion in one dimension.

There are some statistically significant differences in fractal dimension within the data, however. The greatest difference exists between the average and the values along the northernmost transects. Along 48°N, the average slope suggests that the return is patchier than the other lines, and, in fact, it is even slightly patchier than one would expect from a turbulent process. By contrast, the average slope along 47°N suggests that the return there is less patchy than the other lines, with more variability. A smaller, but significant, difference exists between the daytime and nighttime data. The nighttime data are patchier, which might be an effect of the diurnal migration of zooplankton and fish between near-surface waters at night and deeper waters during the day. We speculate that a higher fraction of the scattering at night is caused by fauna, and that this is patchier than scattering from phytoplankton.

There is evidence to support the notion that the distribution of phytoplankton might be less patchy than our lidar data. In an indirect estimate of the patchiness of phytoplankton distribution, Lovejoy *et al.*[4] made airborne measurements of radiance from the ocean in eight channels, and over spatial scales from 14 m to 110 km. The spectral slope for all channels was ~1.25, at least for scales greater than 100 m. Some channels exhibit a flattening at smaller scales, but even the steepest slopes are flatter than our subsurface values. Seuront *et al.*[10] estimated phytoplankton density directly with a fluorometer and calculated the slope of the temporal power spectrum to be ~1.22 for time scales between ~100 and 40,000 s. Assuming Taylor's hypothesis of frozen flow, our smallest spatial scale would be within the same regime as long as the flow is not greater than a few centimeters per second. In contrast to these values, Makris *et al.*[11] measured the distribution of schooling fish and obtained a slope of 1.5. Thus the diurnal migration of fauna might explain the day and night differences in patchiness. Fish and zooplankton are expected to be patchier than phytoplankton, and more of the scattering is likely from these patchier scattering objects at night than during the day, leading to a greater slope at night than during the day.

The lack of a statistically significant difference among the various depths between 5 and 20 m was a surprise. Density profiles of the water column at six stations along

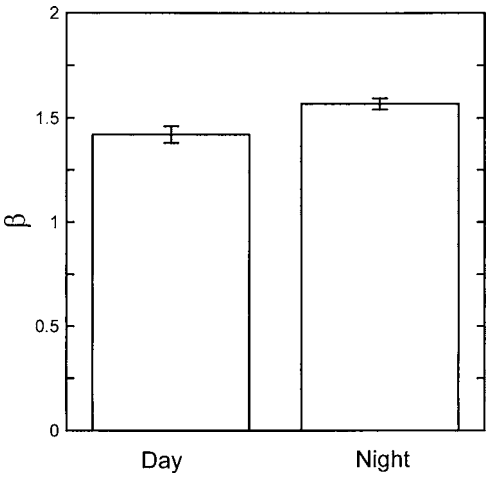

Fig. 5. Day and night values of power spectral slopes of below-surface data (from Table 2).

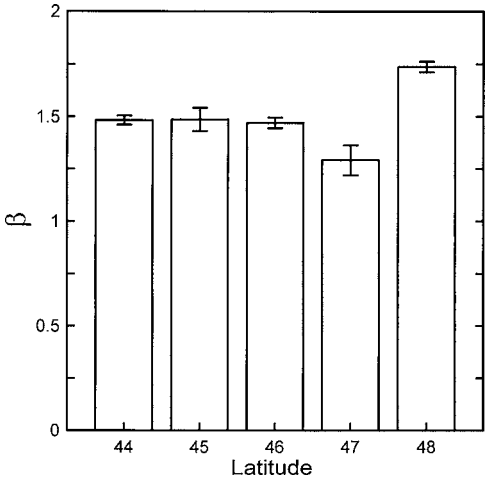

Fig. 6. Latitude dependence of power spectral slopes of below-surface data (from Table 2).

each line were measured from a ship on the same day as the lidar measurements. These showed a well-mixed surface layer with a depth that varied from 3 to 25 m, with an average value of 11.4 m and a standard deviation of 6.4 m. This is within the depth range of our data, and we conclude that there was no statistically significant difference in fractal dimension above and below the pycnocline.

ACKNOWLEDGMENTS

Dave Griffith of the NOAA Southwest Fisheries Science Center provided water column profiles. Holly Sewell used these profiles to estimate mixed-layer depth.

REFERENCES

1. J. Feder, *Fractals* (Plenum, l988).
2. V. V. Zosimov and K. A. Naugolnykh, "Fractal structure of large-scale variability of wind-driven waves according to laser-scanning data," Chaos **4**, 21–24 (1994).
3. J. A. Shaw and J. H. Churnside, "Fractal laser glints from the ocean surface," J. Opt. Soc. Am. A **14**, 1144–1150 (1997).
4. S. Lovejoy, D. Schertzer, Y. Tessier, and H. Gaonac'h, "Multifractals and resolution-independent remote sensing algorithms: the example of ocean colour," Int. J. Remote Sens. **22**, 1191–1234 (2001).
5. J. H. Churnside, J. J. Wilson, and V. V. Tatarskii, "Airborne LIDAR for fisheries applications," Opt. Eng. **40**, 406–414 (2001).
6. E. D. Brown, J. H. Churnside, R. L. Collins, T. Veenstra, J. J. Wilson, and K. Abnett, "Remote sensing of capelin and other biological features in the North Pacific using LIDAR and video technology," ICES J. Mar. Sci. **59**, 1120–1130 (2002).
7. J. H. Churnside, D. A. Demer, and B. Mahmoudi, "A comparison of LIDAR and echosounder measurements of fish schools in the Gulf of Mexico," ICES J. Mar. Sci. **60**, 147–154 (2003).
8. J. H. Churnside and L. A. Ostrovsky, "LIDAR observation of a strongly nonlinear internal wave train in the Gulf of Alaska," Int. J. Remote Sens. **26**, 167–177 (2005).
9. See National Data Buoy Center at http://www.ndbc.noaa.gov/index.shtml.
10. L. Seuront, F. Schmitt, Y. Lagadeuc, D. Schertzer, and S. Lovejoy, "Multifractal analysis of phytoplankton biomass and temperature in the ocean," Geophys. Res. Lett. **23**, 3591–3594 (1996).
11. N. C. Makris, P. Ratilal, D. T. Symonds, S. Jagannathan, S. Lee, and R. W. Nero, "Fish population and behavior revealed by instantaneous continental shelf-scale imaging," Science **311**, 660–663 (2006).